

# Reproducing neutrino effects on the matter power spectrum through a degenerate Fermi gas approach

E. L. D. Perico\*

*Instituto de Física Gleb Wataghin, Universidade Estadual de Campinas,  
PO Box 6165, 13083-970, Campinas, SP, Brasil*

A. E. Bernardini†

*Departamento de Física, Universidade Federal de São Carlos,  
PO Box 676, 13565-905, So Carlos, SP, Brasil*

(Dated: October 11, 2024)

## Abstract

Modifications on the predictions for the matter power spectrum based on the hypothesis of a tiny contribution due to a degenerate Fermi gas (DFG) test fluid in some dominant cosmological backgrounds are investigated. Reporting about the systematic way of accounting for all the cosmological perturbations through the Boltzmann equation, we obtain analytical results for the density fluctuation,  $\delta$ , and the fluid velocity divergence,  $\theta$ , of a DFG test fluid at the radiation-dominated background, through a ultra-relativistic approximation, and at the matter-dominated and  $\Lambda$ -dominated eras, through a non-relativistic approximation. Small contributions to the matter power spectrum are obtained and reproduced by numerical calculations, in order to be compared with those ones for non-relativistic massive and ultra-relativistic massless neutrinos. Lessons concerning the formation of large scale structures of degenerate Fermi fluids are depicted, and consequent deviations from standard  $\Lambda$ CDM predictions for the matter power spectrum (with and without neutrinos) are quantified.

PACS numbers: 98.80.-k, 12.10.-g, 14.60.St, 95.36.+x

---

\*Electronic address: elduarte@ifi.unicamp.br

†Electronic address: alexeb@ufscar.br, alexeb@ifi.unicamp.br

## I. INTRODUCTION

The cosmic accelerated expansion related to the conception of dark energy, the nature of dark matter components, the role of cosmological background neutrinos, and finally, the intrinsic relations among them belong to one of the most challenging frameworks in theoretical physics at present. Such an enlarged overview of the dark sector do necessarily involve a fruitful interplay between general relativity, astrophysics and particle physics [1–4] that are fundamental to the linear perturbation theory that describes the cosmic inventory.

The theory for cosmological perturbations has been highly predictive since it has explained the precision measurements of temperature and polarization anisotropies of the cosmic microwave background (CMB), most notably from the Wilkinson Microwave Anisotropy Probe [5]. Even being a matter of the same scope, the fine-tuning between the theoretical predictions and the observable data for large scale structures still deserves sharper analysis. In fact it falls on more complex procedures for which even the nonlinearity effects are sometimes relevant [6]. The matter power spectrum describes the density contrast of the Universe, which parameterize the inhomogeneities in the matter distribution of the Universe. The density contrast corresponds to the difference between the local density and the averaged density of some energy component of the cosmic inventory. On large scales, gravity competes with cosmic expansion, and structures grow according to the linear theory. On small scales, gravitational collapse is non-linear, and the density contrast can only be computed accurately using N-body simulations.

Beside its intrinsic phenomenological character related to the large scale structures, one of the experimental techniques for determining the mass of the neutrino through cosmological measurements, namely the CMB results, is by inferring the transfer function in the matter power spectrum at small scales [7, 8]. The contribution due to massive neutrinos to the closure fraction of cold dark matter at present can be depicted from the modifications on the matter power spectrum, even for neutrinos behaving like hot dark matter at higher redshifts. It follows that the amount of cold dark matter at earlier epochs should be substantially reduced, suppressing the formation of large scale structures, when it is compared to a situation without massive neutrinos [9–11]. The effects, however, are attenuated in case of hot dark matter or massless neutrinos. A comparison of the observationally-inferred matter power spectrum with the power spectrum expected without the effects of massive

neutrinos allows one to compute the contribution of neutrinos to the cosmic inventory.

The point at our manuscript is that the hypothesis of a tiny fraction of the cosmic inventory evolving cosmologically as a degenerate Fermi gas (DFG) test fluid can mimic the massive neutrino cosmological behavior at several dominant cosmological backgrounds. The approach for treating the cosmological perturbation for ultra-relativistic neutrinos as hot dark matter, in general, differs from the approach for treating non-relativistic neutrinos, as an additional cold dark matter component. Treating massive neutrinos as a DFG not only gives novel ingredients to the recursive idea of a self-gravitating Fermi gas models but also allows for quantifying a smooth transition between ultra-relativistic (UR) and non-relativistic (NR) thermal regimes for neutrinos in the cosmic background. In a previous issue [12], an analytical procedure based on Bianchi identities was adopted for obtaining the evolution of perturbations for a class of relativistic to non-relativistic evolving fluid. Our proposal has become a convenient tool used for describing the role of such particles in the cosmic inventory so that some peculiar modifications on the matter power spectrum can be debugged.

Assuming that the neutrino temperature at present should be of about  $T_{0\nu} \sim 10^{-4}K$  (depending on some phenomenological correspondence with the neutrino mass), and comparing this with a tiny fraction of a DFG test fluid [12] in equilibrium with the radiation background in the beginning of the radiation dominated era [13], one should expect that the DFG's contribution to the matter power spectrum could be of the same order of magnitude of the neutrino's contribution.

Besides theoretical speculations about the existence of some kind of degenerate Fermi gas (DFG) produced in the early universe [14–16], and the idea of a self-gravitating Fermi gas model introduced to explain the puzzling nature of white dwarf stars [17], it may be expected that at some stage of the evolution of the Universe, primordial density fluctuations have become gravitationally unstable forming dense lumps of dark matter. Such possibilities of forming large scale structures thus suggest some meticulous investigation of the behavior of a DFG as a test fluid in the cosmological background of radiation, matter and cosmological constant  $\Lambda$ .

To quantify some analytical aspects related to the DFG approach that we have proposed, which result in fiducial modified predictions for the matter power spectrum of the cosmic inventory, and that is recurrently confirmed by our numerical calculations, our manuscript

was organized as follows. In section II, we report about the formalism of linear perturbations focused on the study of a perfect fluid through the Einstein equations. In section III we obtain some analytical expressions for the density fluctuation,  $\delta$ , and the fluid velocity divergence,  $\theta$ , for a DFG at radiation dominated, matter dominated, and  $\Lambda$  dominated background universe and for the super-horizon radiation-to-matter dominated regime. In particular, we consider the conservation equation for the stress-energy tensor with a vanishing anisotropic stress tensor ( $\sigma$ ). Reporting about the systematic way of accounting for all the cosmological perturbations through the Boltzmann equation, in section IV we quantify the behavior of the inhomogeneities in the Fermi gas at the radiation-dominated era, through an ultra-relativistic analytical approach, and at the matter-dominated and  $\Lambda$ -dominated eras, through a non-relativistic analytical approach. All the analytical results are consistently verified through the numerical calculations described in section V where the DFG contribution to the matter power spectrum is compared with previously obtained numerical solutions where massive neutrinos correspond to tiny fraction of dark matter components. We draw our conclusions in section VI.

## II. COSMOLOGICAL BACKGROUND AND LINEAR PERTURBATIONS

The cosmological evolution of a homogeneous Friedmann-Robertson-Walker (FRW) flat universe with averaged energy density,  $\bar{\rho}(\eta)$ , and averaged pressure,  $\bar{\mathcal{P}}(\eta)$ , is described in terms of the universe scale factor,  $a(\eta)$ , through the following components of the Einstein equation,

$$\left(\frac{da/d\eta}{a}\right)^2 = \frac{8\pi}{3}Ga^2\bar{\rho}, \quad (1)$$

$$\frac{d}{d\eta}\left(\frac{da/d\eta}{a}\right) = -\frac{4\pi}{3}Ga^2(\bar{\rho} + 3\bar{\mathcal{P}}), \quad (2)$$

where  $\eta$  is the conformal time, and  $G$  is the Newtonian constant, and  $c = 1$ .

Reporting about the properties of a perfect fluid, the above elementary textbook equations can be depicted from the conservation properties of a stress-energy tensor  $T_\nu^\mu$  that, at a comoving frame, is given by [10]

$$T^{\mu\nu} = \mathcal{P}g^{\mu\nu} + (\rho + \mathcal{P})U^\mu U^\nu, \quad (3)$$

where  $U$  is the 4-velocity of the fluid particles,  $g_{\mu\nu}$  is the metric tensor, and energy density

and pressure are decomposed into averaged and perturbative values,  $\rho = \bar{\rho} + \delta\rho$  and  $\mathcal{P} = \bar{\mathcal{P}} + \delta\mathcal{P}$ . Once one assumes the validity of the Einstein equation, the corresponding conservation equation for a non-interacting single-particle fluid is thus given in terms of  $T_{;\mu}^{\mu\nu} = 0$ . One shall notice that the collective behavior prescribed by our DFG approach guarantees that the stress-tensor is isotropic and diagonal, and that the energy-momentum tensor can thus be analytically described in terms of the above space-time dependencies.

Throughout our study, we have chosen to work out the perturbation equations for the above scenario in the longitudinal gauge since it has set more simplified connections to preliminary studies on cosmological perturbations [7, 9–11, 18]. By considering that the non-diagonal metric perturbations vanish [11], two scalar degrees of freedom are eliminated from Eq. (3), and the remaining ones are defined in terms of two scalar potentials  $\phi$  and  $\psi$  as

$$g_{\mu 0} = -a^2(1 + 2\psi)\delta_{\mu 0}, \quad g_{ij} = a^2(1 - 2\phi)\delta_{ij}. \quad (4)$$

The Bianchi identities [10] then provide us with the constraints that set the conservation of the stress-energy tensor in the Fourier  $k$ -space, which can be summarized by the continuity equation,

$$\dot{\delta} = -(1 + \omega)(\theta - 3\dot{\phi}) - 3\frac{\dot{a}}{a}(1 + \delta)(1 + \omega) - \frac{\dot{\bar{\rho}}}{\bar{\rho}}(1 + \delta), \quad (5)$$

and by the Euler equation,

$$\dot{\theta} = \frac{k^2 \delta}{1 + \omega} \frac{\delta\mathcal{P}}{\delta\rho} - \sigma k^2 - 4\frac{\dot{a}}{a}\theta + \psi k^2 - \left( \frac{\dot{\bar{\rho}} + \dot{\bar{\mathcal{P}}}}{\bar{\rho}} \right) \frac{\theta}{1 + \omega}, \quad (6)$$

with

$$a\frac{\partial\bar{\rho}}{\partial a} + 3\bar{\rho}(1 + \omega) = 0, \quad (7)$$

where  $\omega = \bar{\mathcal{P}}/\bar{\rho}$ , and  $\theta$ ,  $\delta$  and  $\sigma$  are, respectively, the density fluctuation, the fluid velocity divergence, and the shear stress defined by

$$\delta \equiv \delta\rho/\bar{\rho}, \quad (\bar{\rho} + \bar{\mathcal{P}})\theta \equiv ik^j\delta T_j^0, \quad \text{and} \quad (\bar{\rho} + \bar{\mathcal{P}})\sigma \equiv -\left(\hat{k}^i\hat{k}_j - \frac{1}{3}\delta_j^i\right)\Sigma_i^j, \quad (8)$$

with  $\Sigma_i^j \equiv T_i^j - (\delta_i^j/3)T_k^k$ .

The solutions of Eq. (1) for radiation and matter fluid backgrounds, and for the cosmological constant, with the corresponding equation of state respectively represented by

$\bar{\mathcal{P}}_r = \bar{\rho}_r/3$ ,  $\bar{\mathcal{P}}_m = 0$  and  $\bar{\mathcal{P}}_\Lambda = -\bar{\rho}_\Lambda$ , are given by

$$\bar{\rho}_r = \rho_0 \frac{\Omega_r}{a^4}, \quad \bar{\rho}_m = \rho_0 \frac{\Omega_m}{a^3}, \quad \rho_\Lambda = \rho_0 \Omega_\Lambda, \quad (9)$$

where the scale factor,  $a \equiv a(\eta)$ , during an approach for radiation-to-matter dominated era is given by,

$$a(\eta) \approx \frac{2\pi G \rho_0}{3} \Omega_m \eta^2 + \sqrt{\frac{8\pi G \rho_0}{3} \Omega_r \eta}, \quad (10)$$

and during the  $\Lambda$  dominated era by

$$a(\eta) \approx \left[ 3 \left( \frac{\Omega_\Lambda^{2/6}}{\Omega_m^{1/3}} - \frac{4\sqrt{\Omega_r \Omega_\Lambda}}{\Omega_m} \right) - \sqrt{\frac{8\pi G \rho_0 \Omega_\Lambda}{3} \eta} \right]^{-1}. \quad (11)$$

where  $\rho_0$  is the universe's density at present, and  $\Omega_s = \bar{\rho}_s/\rho_0$ , with  $s = r, m, \Lambda$ .

Finally, by decomposing the Einstein equations into time-time, longitudinal time-space, trace space-space, and longitudinal traceless space-space components, one obtains four equations to the linear perturbations in the  $k$ -space, which through Eq. (4), in terms of  $\phi$  and  $\psi$ , are given by

$$8\pi a^2 G T_0^0 = -3 \left( \frac{\dot{a}}{a} \right)^2 + 6 \frac{\dot{a}}{a} \dot{\phi} + 6 \left( \frac{\dot{a}}{a} \right)^2 \psi + 2k^2 \phi, \quad (12a)$$

$$4\pi G a^2 (\bar{\rho} + \bar{\mathcal{P}}) \theta = k^2 \left( \dot{\phi} + \frac{\dot{a}}{a} \psi \right), \quad (12b)$$

$$\frac{4}{3} \pi G a^2 T_i^i = -\frac{\ddot{a}}{a} + \frac{1}{2} \left( \frac{\dot{a}}{a} \right)^2 + \frac{k^2}{3} (\phi - \psi) + \ddot{\phi} + \frac{\dot{a}}{a} (\dot{\psi} + 2\dot{\phi}) + 2\psi \frac{\ddot{a}}{a} - \psi \left( \frac{\dot{a}}{a} \right)^2, \quad (12c)$$

$$12\pi G a^2 (\bar{\rho} + \bar{\mathcal{P}}) \sigma = k^2 (\phi - \psi). \quad (12d)$$

In the limit of single-particle fluid dominated eras separately described by each element of Eq. (9), and in the absence of the shear stress, i. e.  $\sigma \approx 0$ , one can set  $\psi \approx \phi$  in order to derive some analytic expressions for the evolution of the metric perturbation through the solutions for the scale factor given by Eqs. (10) and (11). The full continuity, Euler and Einstein equations thus result in

$$\phi_r(\eta) = C_1 \frac{\cos \omega + \omega \sin \omega}{\omega^3} + C_2 \frac{\sin \omega - \omega \cos \omega}{\omega^3}, \quad (13a)$$

$$\phi_m(\eta) = -\frac{D_1}{5\omega^5} + D_2, \quad (13b)$$

$$\phi_\Lambda(\eta) = F_1(b - \eta)^3 + F_2(b - \eta), \quad (13c)$$

with  $\omega \equiv k\eta/\sqrt{3}$ . The coefficients with sub-index 1 in the above equations are related to the so-called isentropic decaying modes, in the same fashion that the coefficients with sub-index 2 are related to the isentropic growing modes. As expected, decaying modes are suppressed during the cosmological evolution. In addition, the solution for  $\phi$  at the super-horizon limit during the transitory radiation-to-matter periods is described by

$$\phi(y) = S_1 \frac{\sqrt{1+y}}{y^3} + S_2 \frac{16 + 8y - 2y^2 - 9y^3}{y^3}, \quad (14)$$

where  $y \equiv a/a_{eq} = \bar{\rho}_m/\bar{\rho}_r$ ,  $a_{eq}$  is the scale factor at the time of equality,  $\bar{\rho}_r = \bar{\rho}_m$ , and  $a \equiv a(\eta)$  is given by Eq. (11).

### III. DFG TEST FLUID SOLUTIONS

To obtain analytical solutions for a DFG as a test fluid in some of the cosmological backgrounds briefly discussed in the previous section, we have to follow a sequence of consistent simplifications. Let us consider that the phase space distribution of the particles gives the number of particles in a differential volume  $dx^1 dx^2 dx^3 dp_1 dp_2 dp_3$  in phase space,

$$f(x^i, p_j, \eta) dx^1 dx^2 dx^3 dp_1 dp_2 dp_3 / (2\pi)^3 = dN, \quad (15)$$

with  $p_j \equiv p_j(p, n_j)$ , and where  $f$  is a Lorentz scalar that is invariant under canonical transformations. The general expression for the stress-energy tensor, in case of a single-particle fluid, written in terms of the distribution function  $f$  and of the physical quadrimomentum  $P^\mu$  components, is then given by

$$T_{\mu\nu} = \int \frac{dP_1 dP_2 dP_3}{(2\pi)^3 (-g)^{1/2}} \frac{P_\mu P_\nu}{P^0} f(x^i, p_j, \eta), \quad (16)$$

The phase-space distribution function evolves according to the Boltzmann equation as

$$\frac{Df}{d\eta} = \frac{\partial f}{\partial \eta} + \frac{dx^i}{d\eta} \frac{\partial f}{\partial x^i} + \frac{dq}{d\eta} \frac{\partial f}{\partial q} + \frac{dn_i}{d\eta} \frac{\partial f}{\partial n_i} = \left( \frac{\partial f}{\partial \eta} \right)_C, \quad (17)$$

where, for non-interacting fluids, the right-term (collision term) vanishes. The fluid temperature is, however, not uniform. Thus one conveniently sets  $T = \bar{T} + \delta T$  with  $\delta T = \delta T(x^i, n_j, \eta)$ ,  $a p^i \equiv q^i \equiv q n^i$ , where  $q$  is the comoving momentum, and  $\bar{T}$  is the unique

time-dependent quantity. Expanding the perturbed distribution function,  $f(x^i, p_j(p, n_j), \eta)$ , around the temperature averaged value,  $\bar{T}(\eta)$ , with  $f|_{\bar{T}} = \bar{f}(p, \bar{T}(\eta))$  up to first order terms in  $\delta T$ , as

$$f(x^i, p_j, \eta) \approx f|_{\bar{T}} + \left. \frac{\partial f}{\partial T} \right|_{\bar{T}} \delta T(x^i, n_j, \eta) \equiv \bar{f}(p, \eta) [1 + \Psi(x^i, p_j, \eta)] , \quad (18)$$

the Boltzmann equation in the Fourier  $k$ -space for the longitudinal gauge becomes

$$\frac{\partial \bar{f}}{\partial \eta} (1 + \Psi) + \dot{\Psi} \bar{f} + i \frac{q}{\epsilon} (\vec{k} \cdot \hat{n}) \Psi \bar{f} + (q\dot{\phi} - i\epsilon (\vec{k} \cdot \hat{n})\psi) \frac{\partial \bar{f}}{\partial q} = \left( \frac{\partial \bar{f}}{\partial \eta} \right)_C , \quad (19)$$

where we have rewritten energy and momentum in terms of the (pseudo)comoving energy,  $\epsilon = a E = a(p^2 + m^2)^{1/2} = (q^2 + a^2 m^2)^{1/2}$ , and of the comoving momentum,  $q = p a$ .

In this context, by reducing the notation for the averaged fluid temperature,  $\bar{T}$ , to  $\sim T$ , from this point the distribution function for a DFG can be given by

$$\bar{f}(p, \eta) = g_d \left( \exp \left[ \frac{E - \mu}{T} \right] + 1 \right)^{-1} \approx \begin{cases} g_d & \text{for } E < \mu \\ 0 & \text{for } E > \mu \end{cases} , \quad (20)$$

where  $g_d$  is the number of spin degrees of freedom,  $\mu$  is the chemical potential (that for lower temperatures approximates the Fermi energy  $\mu \xrightarrow{T \rightarrow 0} E_F$ ), and the Planck and the Boltzmann constants,  $\hbar$  and  $k_B$ , were set equal to unity. Reporting about Eq. (16), the pressure and the energy density for a DFG are given by

$$\begin{aligned} \bar{P}_d &= g_d \frac{m^4}{16\pi^2} \left[ \frac{\sqrt{1 + \chi^2}}{\chi^4} \left( \frac{2}{3} - \chi^2 \right) + \ln \frac{1 + \sqrt{1 + \chi^2}}{\chi} \right] , \\ \bar{\rho}_d &= g_d \frac{m^4}{16\pi^2} \left[ \frac{\sqrt{1 + \chi^2}}{\chi^4} (2 + \chi^2) - \ln \frac{1 + \sqrt{1 + \chi^2}}{\chi} \right] , \end{aligned} \quad (21)$$

where  $\chi \equiv (m/q_F)a$ ,  $m$  is the particle mass, and  $q_F$  is the comoving Fermi momentum.

Assuming that the DFG behaves as a test fluid subject to perturbations due to the presence of a background scalar potential,  $\phi$ , the corresponding continuity and Euler equations would be given by

$$\frac{\partial \delta \rho_d}{\partial \eta} = - \frac{m^4}{3\pi^2} \frac{\sqrt{1 + \chi^2}}{\chi^4} (\theta_d - 3\dot{\phi}) - \frac{\dot{a}}{a} \delta \rho_d \frac{4 + 3\chi^2}{1 + \chi^2} , \quad (22a)$$

$$\dot{\theta}_d + \sigma_d k^2 + \frac{\dot{a}}{a} \frac{\theta_d}{1 + \chi^2} - \phi k^2 = \delta \rho_d \frac{k^2 \chi^4 \pi^2}{m^4 (1 + \chi^2)^{3/2}} . \quad (22b)$$

where the index  $d$  stands for the DFG. Supposing that the DFG averaged density is equivalent to the averaged density of massive neutrinos, and considering that neutrinos are ultra-relativistic only deep inside the radiation dominated era, we can approximate the above equations by setting  $\chi \ll 1$  during the radiation dominated era and  $\chi > 1$  after the radiation-to-matter equilibrium, i. e. at  $a = a_{eq}$ .

### A. Radiation-to-matter period for very large scales

For  $k\eta \ll 1$  and with vanishing  $\sigma$ , Eq. (22) becomes

$$\frac{\partial \ln [\chi(\bar{\rho}_d + \bar{\mathcal{P}}_d)\theta_d]}{\partial \ln \chi} = -3, \quad (23a)$$

$$\chi \frac{\partial}{\partial \chi} \delta\rho_d - \frac{m^4}{\pi^2} \frac{\sqrt{1+\chi^2}}{\chi^3} \frac{\partial \phi}{\partial \chi} + \delta\rho_d \frac{4+3\chi^2}{1+\chi^2} = 0. \quad (23b)$$

Using the analytical solution for  $\phi$  in case of super-horizon scales (c. f. Eq. (14)) one thus obtains

$$\theta_d = \frac{\pi^2}{m^4} \frac{3}{\sqrt{1+\chi^2}} S_0, \quad (24)$$

$$\delta_d = 8 \left[ S_1 \frac{\sqrt{1+y}}{y^3} + S_2 \frac{16+8y-2y^2}{y^3} + S_4 \right] \left[ (2+\chi^2) - \frac{\chi^4}{\sqrt{1+\chi^2}} \operatorname{arccsch} \chi \right]^{-1}. \quad (25)$$

where  $S_i$ , with  $i = 0, 1, 2, 3$ , are constants used to independently match separated solutions for radiation and matter dominated eras. Although the density contrast for CDM and photons remains the same for the period of radiation-to-matter transition, Fig. 1 shows that the DFG density contrast does not reach the growing rate of the CDM density contrast at the end of the matter dominated era for super-horizon scales. We shall see that such a behavior recurrently happens at scales  $\gtrsim Mpc/h$ , with a non-trivial contribution to the matter power spectrum today.

### B. Radiation dominated era

For the radiation dominated era with vanishing  $\sigma$ , the components of Eq. (22) can be approximated by

$$\dot{\delta}_d = -\frac{4}{3}\theta_d + 4\dot{\phi}, \quad \text{and} \quad \dot{\theta}_d = k^2 \frac{1}{4}\delta_d + k^2 \phi. \quad (26)$$

Using the analytical solution for  $\phi_r$  from Eq. (13a) one thus obtains

$$\delta_d = 2C_1 \frac{2(1 - \omega^2) \cos \omega + \omega(2 - \omega^2) \sin \omega}{\omega^3} + 2C_2 \frac{2(1 - \omega^2) \sin \omega - \omega(2 - \omega^2) \cos \omega}{\omega^3}, \quad (27a)$$

$$\theta_d = \frac{\sqrt{3}}{2} C_1 \frac{(\omega^2 - 2) \cos \omega - 2\omega \sin \omega}{\omega^2} + \frac{\sqrt{3}}{2} C_2 \frac{(\omega^2 - 2) \sin \omega + 2\omega \cos \omega}{\omega^2}. \quad (27b)$$

where  $C_i$ , with  $i = 1, 2$ , are also fitting constants. In this case the DFG perturbation reproduces the same behavior of radiation perturbations since, for a ultra-relativistic condition, one considers  $\chi \ll 1$ . The solutions for the growing mode related to the coefficient  $C_2$  correspond to oscillating perturbations once the non-vanishing pressure has prejudiced the gravitational collapse.

### C. Matter dominated era

Deep inside the matter dominated era, when  $\rho_{cr} \approx \bar{\rho}_m$ , with vanishing  $\sigma$ , the components of Eq. (22) become

$$\dot{\delta}_d = -\theta_d + 3\dot{\phi}, \quad \text{and} \quad \dot{\theta}_d = \frac{k^2 \delta_d}{5\chi^2} - k^2 \sigma_d + k^2 \psi. \quad (28)$$

Using the analytical solution for  $\phi_m$  from Eq. (13b) one finally obtains

$$\begin{aligned} \delta_d = & D_1 \frac{12\sqrt{3}c_m^2}{k^9\eta} \left[ \frac{k^4}{5} - 12\frac{k^2}{\eta^2} + 96c_m^2 \right] - D_2 \frac{k^2 \eta^2}{6} + D_3 \cos \frac{\sqrt{3}k}{2c_m \eta} - D_4 \sin \frac{\sqrt{3}k}{2c_m \eta} \\ & - D_2 \frac{k^4}{8c_m^2} \left[ \cos \frac{\sqrt{3}k}{2c_m \eta} \text{Ci} \frac{\sqrt{3}k}{2c_m \eta} + \sin \frac{\sqrt{3}k}{2c_m \eta} \text{Si} \frac{\sqrt{3}k}{2c_m \eta} \right], \end{aligned} \quad (29)$$

and

$$\begin{aligned} \theta_d = & \left\{ D_1 \frac{9\sqrt{3}}{k^9} \left[ \frac{6k^4}{\eta^4} - \frac{96k^2 c_m^2}{\eta^2} + \frac{8k^4 c_m^2}{15} + 256c_m^4 \right] - D_3 \frac{\sqrt{3}k}{c_m} \sin \frac{\sqrt{3}k}{2c_m \eta} - D_4 \frac{\sqrt{3}k}{c_m} \cos \frac{\sqrt{3}k}{2c_m \eta} \right. \\ & \left. + D_2 \frac{\sqrt{3}k^5}{8c_m^3} \left[ \text{Ci} \frac{\sqrt{3}k}{2c_m \eta} \sin \frac{\sqrt{3}k}{2c_m \eta} - \text{Si} \frac{\sqrt{3}k}{2c_m \eta} \cos \frac{\sqrt{3}k}{2c_m \eta} \right] + D_2 \frac{k^2 \eta}{c_m^2} \left[ \frac{k^2}{4} + \frac{2\eta^2 c_m^2}{3} \right] \right\} \frac{1}{2\eta^2}, \end{aligned} \quad (30)$$

where  $c_m = (G \rho_0 m \pi \Omega_m)/q_F$ , and  $\text{Si}(z)$  and  $\text{Ci}(z)$  are the integral sine and cosine functions. The term proportional to  $\frac{k^2 \eta^2}{6}$  at Eq. (29) shows that the density contrast,  $\delta$ , grows at the same rate as the expansion parameter,  $a$ . The last term between brackets oscillates as  $\sin(\sqrt{3}k/(2c_m \eta))$  for  $\eta < \sqrt{3}k/(2c_m)$ , after which, it presents a logarithmic growing dependence on the conformal time,  $\eta$ . Turning to the solution for the fluid velocity divergence,  $\theta$ ,

described by Eq. (30), the terms inside the first brackets describe damped oscillations which are similar to those parameterized by  $\sin(\sqrt{3}k/(2c_m \eta))$  at Eq. (29). For  $\eta < \sqrt{3}k/(2c_m)$ , the decreasing amplitude is proportional to the inverse of the expansion parameter, i. e.  $1/a$ , after which the oscillating behavior is completely suppressed. The last term in the brackets presents a linear growing dependence on the conformal time,  $\eta \propto \sqrt{a}$ .

In general lines, the perturbations described by Eqs. (29) and (30) present oscillating behavior at the beginning of the matter dominated era up to the point where it is suppressed by the subsequent growing modes. The complete solutions for  $\delta$  and  $\theta$  can be depicted from Figs. 2 and 3, from which one can notice that DFG perturbations never reach the same growing rate of CDM perturbations.

#### D. Cosmological constant dominated era

If one assumes the non-relativistic dynamics for a DFG test fluid at late times, that happens when one sets  $\chi \gg 1$  at Eq. (21), the cosmological constant era can be reproduced by the same dynamics that drive the perturbations into the matter dominated era, (c. f. Eq. (28)). Using the analytical solution for  $\phi_\Lambda$  from Eq. (13c) one thus obtains the density contrast,

$$\begin{aligned} \delta_d = & 3F_1 c_\chi^2 (b - \eta) + F_3 \cos \left[ \frac{\pi \eta (2b - \eta)}{2 c_\Lambda^2} \right] + F_4 \sin \left[ \frac{\pi \eta (2b - \eta)}{2 c_\Lambda^2} \right] \\ & + 3c_\Lambda \{ F_2 + F_1 c_\chi^2 \} \left\{ \cos \left[ \frac{\pi}{2} z^2 \right] \text{Fc} [z] + \sin \left[ \frac{\pi}{2} z^2 \right] \text{Fs} [z] \right\} \\ & + \frac{c_\Lambda^3}{\pi} \{ F_2 k^2 - 9F_1 \} \left\{ \cos \left[ \frac{\pi}{2} z^2 \right] \text{Fs} [z] - \sin \left[ \frac{\pi}{2} z^2 \right] \text{Fc} [z] \right\}, \end{aligned} \quad (31)$$

where  $z \equiv (b - \eta)/c_\Lambda$ ,  $c_\Lambda^2 \equiv \sqrt{3} c m \pi / k q_F$ ,  $c_\chi \equiv c m / q_F$ ,  $\text{Fs}(z)$  and  $\text{Fc}(z)$  are respectively the Fresnel integral sine and cosine functions, and the  $c$  and  $b$  are constants given by

$$c = \sqrt{\frac{3}{8\pi G \rho_0 \Omega_\Lambda}}, \quad b = 3 \sqrt{\frac{3}{8\pi G \rho_0} \left( \frac{1}{\Omega_m^{1/3} \Omega_\Lambda^{1/6}} - \frac{4\Omega_r^{1/2}}{\Omega_m} \right)}, \quad (32)$$

The solution for the fluid velocity divergence in correspondence to the above density contrast is

$$\begin{aligned}
\theta_d = & -9F_1(\eta - b)^2 + F_3 \frac{\pi}{c_\Lambda} z \cos \left[ \frac{\pi \eta(2b - \eta)}{2 c_\Lambda^2} \right] - F_4 \frac{\pi}{c_\Lambda} z \sin \left[ \frac{\pi \eta(2b - \eta)}{2 c_\Lambda^2} \right] \\
& - \left\{ \cos \left[ \frac{\pi}{2} z^2 \right] \text{Fc} [z] + \sin \left[ \frac{\pi}{2} z^2 \right] \text{Fs} [z] \right\} \{ F_2 k^2 - 9F_1 \} c_\Lambda^2 z \\
& + \left\{ \cos \left[ \frac{\pi}{2} z^2 \right] \text{Fs} [z] - \sin \left[ \frac{\pi}{2} z^2 \right] \text{Fc} [z] \right\} \left\{ F_2 \frac{3\pi}{c_\Lambda} + F_1 \sqrt{3} k c_\Lambda c_\chi \right\} c_\Lambda z.
\end{aligned} \tag{33}$$

These solutions correspond to decreasing functions that result on decaying modes of perturbation, an effect that match the dynamics ruled by the negative pressure of the dominant fluid.

#### IV. BOLTZMANN EQUATION SOLUTIONS FOR A DFG

In certain sense, the thermodynamics of a DFG is driven by the cosmological behavior of the chemical potential,  $\mu \sim \mu(a)$ . However, depending on its effective contribution to the fluid dynamics, which sometimes is not relevant, additional contributions to the analytical characteristic of the distribution function are usually discarded, i. e. by setting  $\mu = 0$ . That is not the case of our approach, since we are interested in depicting the cosmological behavior of a DFG. The simplest way to consistently include the chemical potential in the following calculations is through the zero order Boltzmann equation for a non-interacting fluid (c. f. Eq. (19)) as

$$0 = \frac{d\bar{f}}{d\eta} = \dot{a} \frac{\partial \bar{f}}{\partial a} \propto \frac{\partial}{\partial a} \left( \frac{E - \mu}{\bar{T}} \right), \tag{34}$$

from which the last equality sets the constraint among the energy,  $E$ , the temperature,  $T$ , and the chemical potential,  $\mu$ .

The condition given by the above equation results in the following constraint for the dependence of the distribution function on the temperature,

$$\left. \frac{\partial f}{\partial T} \right|_{\bar{T}} = \frac{aE}{p} \frac{\mu - E}{\bar{T}} \frac{\partial \bar{f}}{\partial q} = \frac{\epsilon}{q} \frac{\nu - \epsilon}{\bar{T}} \frac{\partial \bar{f}}{\partial q}, \tag{35}$$

with  $\nu = a\mu$ , a kind of comoving description for  $\mu$ . It allows one to identify the first order perturbation coefficient,  $\Psi$ , that appears in Eq. (18), as

$$\Psi(x^i, n_j, \eta) = \frac{\epsilon(\nu - \epsilon)}{q^2} \frac{\partial \ln \bar{f}}{\partial \ln q} \Delta(x^i, n_j, \eta), \tag{36}$$

where  $\Delta \equiv \delta T/\bar{T}$ . By substituting the above expression for  $\Psi$  into Eq. (19), the Boltzmann equation can be reduced to

$$\frac{\partial}{\partial \eta} \left( \frac{\epsilon(\nu - \epsilon)}{q} \frac{\partial \bar{f}}{\partial q} \Delta \right) + i(\vec{k} \cdot \hat{n})(\nu - \epsilon) \frac{\partial \bar{f}}{\partial q} \Delta + \left( q\dot{\phi} - i(\vec{k} \cdot \hat{n})\epsilon\phi \right) \frac{\partial \bar{f}}{\partial q} = 0, \quad (37)$$

where  $\Delta(x^i, n_j, \eta)$  reads  $\mathcal{D}(k^i, n_j, \eta)$  in the Fourier  $k$ -space as

$$\Delta(x^i, n_j, \eta) = \frac{1}{(2\pi)^3} \int dk^3 \exp[ik_i x^i] \mathcal{D}(k^i, n_j, \eta). \quad (38)$$

The dimensionality of the problem can be reduced by noticing that the evolution of Eq.(37) depends on the direction  $\hat{n}$  through the angle related to  $\hat{k} \cdot \hat{n} = \cos \varphi$ , which is a natural consequence of the isotropy of the homogeneous background.

Performing the  $P_l$ -Legendre expansion with respect to  $\cos(\varphi)$ , one obtains

$$\mathcal{D}(k^i, n_j, \eta) = \sum_{l=0}^{\infty} (-i)^l (2l+1) \Delta_l(k, \eta) P_l(\cos(\varphi)), \quad (39)$$

that results in

$$\Delta_0 = \frac{1}{4\pi} \int d\Omega \mathcal{D}, \quad \Delta_1 = \frac{i}{4\pi} \int d\Omega \cos \varphi \mathcal{D} \quad \text{and} \quad \Delta_2 = -\frac{3}{8\pi} \int d\Omega \left( \cos^2 \varphi - \frac{1}{3} \right) \mathcal{D}, \quad (40)$$

for the first three multipole coefficients. The corresponding evolution equations for the multipole coefficients,  $\Delta_l(k, \eta)$ , are obtained through the integration of the Boltzmann equation (37) multiplied by  $P_l(\hat{k} \cdot \hat{n}) \equiv P_l(\cos \varphi)$  over the solid angle  $d\Omega \equiv d\theta d(\cos \varphi)$ , that results in

$$\begin{aligned} \frac{\partial}{\partial \eta} \left( \frac{\epsilon(\nu - \epsilon)}{q} \frac{\partial \bar{f}}{\partial q} \Delta_0 \right) + (\nu - \epsilon) \frac{\partial \bar{f}}{\partial q} k \Delta_1 + q \frac{\partial \bar{f}}{\partial q} \dot{\phi} &= 0, \\ \frac{\partial}{\partial \eta} \left( \frac{\epsilon(\nu - \epsilon)}{q} \frac{\partial \bar{f}}{\partial q} \Delta_1 \right) - (\nu - \epsilon) \frac{\partial \bar{f}}{\partial q} \frac{k}{3} (\Delta_0 - 2\Delta_2) + \epsilon \frac{\partial \bar{f}}{\partial q} \frac{k}{3} \phi &= 0, \\ \frac{\partial}{\partial \eta} \left( \frac{\epsilon(\nu - \epsilon)}{q} \frac{\partial \bar{f}}{\partial q} \Delta_l \right) + (\nu - \epsilon) \frac{\partial \bar{f}}{\partial q} \frac{k}{2l+1} [(l+1) \Delta_{l+1} - l \Delta_{l-1}] &= 0, \quad \text{for } l \geq 2. \end{aligned} \quad (41)$$

The perturbations for the stress-energy tensor from Eq. (16) can thus be rewritten as

$$\begin{aligned}
\delta\rho_d &= \frac{\Delta_0}{2\pi^2 a^4} \int dq q \epsilon^2 (\nu - \epsilon) \frac{\partial \bar{f}}{\partial q}, \\
\delta\mathcal{P}_d &= \frac{\Delta_0}{6\pi^2 a^4} \int dq q^3 (\nu - \epsilon) \frac{\partial \bar{f}}{\partial q}, \\
\theta_d(\bar{\rho}_d + \bar{\mathcal{P}}_d) &= \frac{\Delta_1}{2\pi^2 a^4} \int dq q^2 \epsilon (\nu - \epsilon) \frac{\partial \bar{f}}{\partial q}, \\
\sigma_d(\bar{\rho}_d + \bar{\mathcal{P}}_d) &= -\frac{\Delta_2}{3\pi^2 a^4} \int dq q^3 (\nu - \epsilon) \frac{\partial \bar{f}}{\partial q},
\end{aligned} \tag{42}$$

and finally, after integrating Eqs. (41) over  $q$  and using the results from Eq. (42), one can resolve the system of equations and find the temporal behavior of the DFG perturbations. From such results we shall verify that it is possible to analytically depict DFG transitory regimes, from relativistic to non-relativistic dynamics.

### A. Ultra-relativistic DFG during the radiation dominated era

When particles are ultra-relativistic, i. e.  $\epsilon = q$ , and  $\nu$  is set equal to zero, the above results should be reduced to that obtained for massless particles [10, 11]. Differently from which is observed when one sets the ultra-relativistic approximation to  $f$ , the spectrum does not remain Planckian when  $\nu \neq 0$ . The  $q$ -integration can be performed separately and the dependence on  $x^i$ ,  $n_j$  and  $\eta$  is kept active. The cosmological behavior of the temperature depicted from Eq. (17) is given by  $T(\eta) \sim T_0 m/[a(\eta) q_F]$  since the energy,  $E$ , is approximated by its ultra-relativistic dependence on the momentum ( $\sim p$ ) through the relation

$$\frac{E - \mu}{T} \approx q_F \frac{q - q_F}{m T_0}, \tag{43}$$

where  $T_0$  is the fluid temperature at present. By performing the quoted integrations for Eqs. (41), the  $\Delta_l$  multipole evolution equations become

$$\dot{\Delta}_0 + k\Delta_1 - \dot{\phi} c_F = 0, \tag{44}$$

$$\dot{\Delta}_1 - \frac{k}{3}(\Delta_0 - 2\Delta_2) - \frac{k}{3}\dot{\phi} c_F = 0, \tag{45}$$

and

$$\dot{\Delta}_l + \frac{k}{2l+1} [(l+1)\Delta_{l+1} - l\Delta_{l-1}] = 0, \quad \text{for } l \geq 2, \tag{46}$$

where  $c_F \equiv q_F^2/(m T_0 \ln(2))$ . By considering the analytical solution for  $\phi_r$  from Eq. (13a), and assuming that the contribution from higher order multipoles  $\Delta_l$ , with  $l \geq 2$ , are suppressed, the above equations lead to

$$\Delta_0 = \frac{C_1 c_F}{\omega^3} [\cos \omega (1 - \omega^2) + \omega \sin \omega] + \frac{C_2 c_F}{\omega^3} [\sin \omega (1 - \omega^2) - \omega \cos \omega] + C_3 \cos \omega - C_4 \sin \omega, \quad (47)$$

and

$$\Delta_1 = -\frac{C_1 c_F}{\sqrt{3}\omega^2} [\cos \omega + \omega \sin \omega] - \frac{C_2 c_F}{\sqrt{3}\omega^2} [\sin \omega - \omega \cos \omega] + \frac{C_3}{\sqrt{3}} \sin \omega + \frac{C_4}{\sqrt{3}} \cos \omega. \quad (48)$$

The above results can be substituted into the integrals from Eqs. (42) in order to give

$$\delta_d \approx 2^4 \pi^3 \ln(2) \frac{m T_0}{q_F^2} \Delta_0, \quad (49)$$

$$\frac{\delta \mathcal{P}_d}{\delta \rho_d} \approx \frac{1}{3}, \quad (50)$$

$$\theta_d \approx 12 \pi^3 \ln(2) \frac{m T_0}{q_F^2} k \Delta_1, \quad (51)$$

and, eventually,

$$\sigma_d \approx -2^3 \pi^3 \ln(2) \frac{m T_0}{q_F} \Delta_2. \quad (52)$$

that reproduce the results from Eqs. (27a) and (27b) obtained through the continuity and Euler equations, i. e. Eqs. (29) and (30), since we have assumed that the DFG behaves as an ideal fluid.

## B. Non relativistic DFG during the matter dominated era

Deep inside the matter era, when  $\rho_{cr} \approx \bar{\rho}_m$ , the cosmological behavior of the temperature depicted from Eq. (17) is given by  $T(\eta) \sim T_0 a(\eta)^{-2}$  since the energy,  $E$ , is approximated by its non-relativistic dependence on the momentum ( $\sim p^2/(2m)$ ) through the relation

$$\frac{E - \mu}{T} \approx \frac{q^2 - q_F^2}{2m T_0}. \quad (53)$$

By performing the quoted integrations of Eqs. (41) over the momentum  $q$ , and assuming that  $\Delta_l \sim 0$ , for  $l \geq 2$ , the multipole evolution equations can be written as

$$\dot{\Delta}_0 + \frac{k}{\chi} \Delta_1 - c_F \dot{\phi} = 0, \quad (54)$$

$$\dot{\Delta}_1 - \frac{k}{3\chi} (\Delta_0 - 2\Delta_2) - \frac{k}{3} \chi c_F \phi = 0, \quad (55)$$

and

$$\dot{\Delta}_l + \left( \frac{k}{2l+1} \right) \frac{1}{\chi} [(l+1)\Delta_{l+1} - l\Delta_{l-1}] = 0, \quad \text{for } l \geq 2. \quad (56)$$

By substituting the analytical solution for  $\phi_m$  from Eq. (13b) into Eqs. (54-55), one obtains

$$\begin{aligned} \Delta_0 = & D_1 c_F \frac{4\sqrt{3}c_m^2}{k^9\eta} \left[ \frac{k^4}{5} - 12 \frac{k^2}{\eta^2} + 96c_m^2 \right] + D_3 \cos \frac{\sqrt{3}k}{2c_m\eta} - D_4 \sin \frac{\sqrt{3}k}{2c_m\eta} \\ & - D_2 c_F \frac{k^4}{24c_m^2} \left[ \cos \frac{\sqrt{3}k}{2c_m\eta} \text{Ci} \frac{\sqrt{3}k}{2c_m\eta} + \sin \frac{\sqrt{3}k}{2c_m\eta} \text{Si} \frac{\sqrt{3}k}{2c_m\eta} \right] - D_2 c_F \frac{k^2 \eta^2}{18}, \end{aligned} \quad (57)$$

$$\begin{aligned} \Delta_1 = & D_1 c_F \frac{\sqrt{3}c_m}{k^{10}} \left[ \frac{6k^4}{\eta^4} - \frac{96k^2 c_m^2}{\eta^2} + \frac{8k^4 c_m^2}{15} + 256c_m^4 \right] - \frac{D_3}{\sqrt{3}} \sin \frac{\sqrt{3}k}{2c_m\eta} - \frac{D_4}{\sqrt{3}} \cos \frac{\sqrt{3}k}{2c_m\eta} \\ & + D_2 c_F \frac{k^4/\sqrt{3}}{24c_m^2} \left[ \text{Ci} \frac{\sqrt{3}k}{2c_m\eta} \sin \frac{\sqrt{3}k}{2c_m\eta} - \text{Si} \frac{\sqrt{3}k}{2c_m\eta} \cos \frac{\sqrt{3}k}{2c_m\eta} \right] + D_2 c_F \frac{k\eta}{9c_m} \left[ \frac{k^2}{4} + \frac{2\eta^2 c_m^2}{3} \right], \end{aligned} \quad (58)$$

where  $c_m \equiv (G \rho_0 m \pi \Omega_m)/q_F$  as it was previously defined. Performing the integrations prescribed by Eqs.(42) and using the non relativistic approximation for the DFG through Eq. (53), the perturbations for the stress-energy tensor are given by

$$\delta_d \approx 12\pi^3 \ln(2) \frac{m T_0}{q_F^2} \Delta_0, \quad (59)$$

$$\frac{\delta \mathcal{P}_d}{\delta \rho_d} \approx \frac{1}{3\chi^2}, \quad (60)$$

$$\theta_d \approx 12\pi^3 \ln(2) \frac{m T_0}{q_F^2} \frac{\Delta_1}{\chi}, \quad (61)$$

and, where required,

$$\sigma_d \approx 8\pi^3 \ln(2) \frac{m T_0}{q_F^2} \frac{\Delta_2}{\chi}. \quad (62)$$

Again the above solutions reproduce the same behavior of the solutions in Eqs. (29) and (30) for an ideal fluid approach. One should notice that the non-null perturbation on the averaged pressure, as obtained through the ideal fluid approach, explains some small deviations from pure cold matter perturbations, for which the pressure vanishes.

### C. Non-relativistic DFG during the $\Lambda$ dominated era

As we have stated in the previous section, when one assumes the non-relativistic dynamics for a DFG test fluid at late times by setting  $\chi \gg 1$  at Eq. (21), the dynamics for the

cosmological constant era can be reproduced by the same equations of matter perturbations. In this case, it is reproduced by Eqs. (54-56). By following the same procedure as for matter and radiations dominated eras, i. e. using the analytical solution for  $\phi_\Lambda$  from Eq. (13c) into Eqs. (54-56), with  $\Delta_l \sim 0$ , for  $l \geq 2$ , one obtains

$$\begin{aligned} \Delta_0 = & F_1 c_F c_\chi^2 (\eta - b) + F_3 \cos \left[ \frac{\pi \eta (2b - \eta)}{2 c_\Lambda^2} \right] + F_4 \sin \left[ \frac{\pi \eta (2b - \eta)}{2 c_\Lambda^2} \right] \\ & + \left\{ \cos \left[ \frac{\pi}{2} z^2 \right] c[z] + \sin \left[ \frac{\pi}{2} z^2 \right] s[z] \right\} c_F c_\Lambda \{ F_2 + F_1 c_\chi^2 \} \\ & + \left\{ \cos \left[ \frac{\pi}{2} z^2 \right] s[z] - \sin \left[ \frac{\pi}{2} z^2 \right] c[z] \right\} c_F \left\{ F_2 c_\chi^{3/2} \sqrt{\frac{k\pi}{\sqrt{3}}} - F_1 c_\Lambda^3 \frac{3}{\pi} \right\}, \end{aligned} \quad (63)$$

$$\begin{aligned} \Delta_1 = & -F_1 c_F c_\chi^2 \frac{\sqrt{3}}{\pi} (b - \eta) + \frac{F_3}{\sqrt{3}} \cos \left[ \frac{\pi \eta (2b - \eta)}{2 c_\Lambda^2} \right] - \frac{F_4}{\sqrt{3}} \sin \left[ \frac{\pi \eta (2b - \eta)}{2 c_\Lambda^2} \right] \\ & - \left\{ \cos \left[ \frac{\pi}{2} z^2 \right] Fc[z] + \sin \left[ \frac{\pi}{2} z^2 \right] Fs[z] \right\} \left\{ F_2 c_\chi^{3/2} \frac{\sqrt{k\pi}}{3^{3/4}} - F_1 c_\Lambda^3 \frac{\sqrt{3}}{\pi} \right\} c_F \\ & + \left\{ \cos \left[ \frac{\pi}{2} z^2 \right] Fs[z] - \sin \left[ \frac{\pi}{2} z^2 \right] Fc[z] \right\} \{ F_2 + F_1 c_\chi^2 \} \frac{c_F c_\Lambda}{\sqrt{3}}. \end{aligned} \quad (64)$$

with  $c_\Lambda^2 \equiv \sqrt{3} c m \pi / (k q_F)$ ,  $c_\chi \equiv c m / q_F$ , and where  $c$  and  $b$  is given by Eq. (32).

Since the Eqs. (59-62) are still valid the DFG perturbations during the  $\Lambda$  dominated era (obtained using the Boltzmann equation) are equivalent to the solutions obtained using Eqs. (31) and (33).

## V. NUMERICAL SOLUTION

Herewith we shall consider the numerical procedures for treating perturbations valid for test fluids in a DFG regime. For such a purpose we have run the public code CAMB [19] based on the synchronous gauge scalar perturbations on the flat Friedmann-Robertson-Walker metric with isentropic initial conditions for the stress-energy perturbations. As one shall notice, the numerical results here obtained are in complete agreement with the preliminary analytical studies that we have proposed in the previous sections.

Considering that the perturbed flat Friedmann-Robertson-Walker metric in the synchronous gauge is described by

$$ds^2 = a^2 \left[ -d\eta^2 + (\delta_{ij} + h_{ij}) dx^i dx^j \right], \quad (65)$$

the continuity and Euler equations of the stress-energy tensor for ideal fluids can be written as

$$\frac{\partial \delta \rho}{\partial \eta} = -\dot{\bar{\rho}} - (\bar{\rho} + \bar{\mathcal{P}}) \left( \theta + \frac{\dot{h}}{2} + 3\frac{\dot{a}}{a} \right) - 3\frac{\dot{a}}{a} \delta \rho \left( 1 + \frac{\delta \mathcal{P}}{\delta \rho} \right), \quad (66)$$

and

$$\left( \dot{\theta} + \sigma k^2 + 4\frac{\dot{a}}{a} \theta \right) (\bar{\rho} + \bar{\mathcal{P}}) + \theta \left( \dot{\bar{\rho}} + \dot{\bar{\mathcal{P}}} \right) = \delta \rho k^2 \frac{\delta \mathcal{P}}{\delta \rho}, \quad (67)$$

with  $h \equiv h_{ii}$ . In analogy to Eq. (21), one thus has

$$\frac{\partial \delta \rho}{\partial \eta} = -\frac{m^4 \sqrt{1 + \chi^2}}{\pi^2 3\chi^4} \left( \theta + \frac{\dot{h}}{2} \right) - \delta \rho \frac{\dot{a} 4 + 3\chi^2}{a 1 + \chi^2}, \quad (68a)$$

and

$$\dot{\theta} + \sigma k^2 + \theta \frac{\dot{a}}{a} \frac{2\chi^2}{1 + \chi^2} = \delta \rho \frac{\chi^4 k^2 \pi^2}{m^4 (1 + \chi^2)^{3/2}}. \quad (68b)$$

We have performed the numerical calculations to obtain the time dependence of the DFG perturbation by introducing the constraints given by Eq.(68) into the CAMB code, with  $\sigma_d \approx 0$ .

### A. Background and perturbation initial conditions

To compare DFG with massive neutrino perturbations in the background of the  $\Lambda$ CDM model, we have set coincident values for the averaged densities of both fluids as preliminary conditions, at early times (radiation dominated) and at very late times (matter era). To obtain the comoving Fermi momentum  $q_F$  for a DFG, we have considered that the ultra-relativistic limit of Eq. (21),

$$\bar{\rho}_d(\chi \ll 1) \approx \frac{m^4 g_d}{8\pi^2 \chi^4} = \frac{g_d q_F^4}{4\pi^2 a^4}, \quad (69)$$

does not depend on the mass,  $m$ . By equating the averaged densities of both matter components as  $\bar{\rho}_d = \bar{\rho}_\nu$  (assuming three degenerated families for each one of them), one easily verifies that

$$\bar{\rho}_d(\chi \ll 1) = \bar{\rho}_\nu(a \ll a_{eq}) = 3\frac{7}{8} \left( \frac{4}{11} \right)^{4/3} \bar{\rho}_\gamma(a), \quad (70)$$

which results in  $q_F \approx 3.65 \cdot 10^{-4} eV/c$ .

By introducing such value into the non-relativistic approximations for the DFG averaged density,

$$\bar{\rho}_d(\chi \gg 1) \approx \frac{m^4 g_d}{6\pi^2 \chi^3} = \frac{g_d q_F^3}{6\pi^2 a^3} m, \quad (71)$$

and following the same equality,  $\bar{\rho}_d = \bar{\rho}_\nu$ , in the limit where  $a$  tends to unity at present,

$$\bar{\rho}_d(\chi \gg 1) = \bar{\rho}_\nu(a \rightarrow 1) = \rho_0 \frac{\Omega_\nu}{a^3}, \quad (72)$$

one can easily depict a “neutrino” mass given by  $m \approx 0.24 eV/c^2$ .

Finally, integrating the isentropic initial conditions over  $q$  for the multipole expansion of the massive neutrino perturbations [10], and using the DFG phase-space distribution, we obtain the same initial conditions for the DFG perturbations and for massless neutrinos.

Fig. 4 shows the density contrast,  $\delta$ , that we have obtained for a DFG. During the radiation dominated era ( $a \ll a_e \approx 2,7 \cdot 10^{-4}$ ) the DFG density contrast  $\delta_d$  has the same oscillating behavior of radiation perturbations,  $\delta_\gamma$ , since both fluids have approximately the same evolution equations. It occurs for a DFG approximated by ultra-relativistic conditions. During the matter dominated era the DFG density contrast oscillates up to the beginning of the non-relativistic regime. After transiting to the non-relativistic scenario, the DFG density contrast oscillating modes are suppressed and the growing modes reproduce the same behavior of CDM perturbation. Finally, when the universe pass to the  $\Lambda$  dominated era, the DFG density contrast growing modes are suppressed by the negative pressure of the dominant fluid.

Fig. 5 allows us to depict the difference between the density contrast of a DFG, for which we have suppressed the higher order multipoles, and the density contrast of massive neutrinos evaluated numerically. The time evolution of the perturbations for both fluids has two fundamental differences. Firstly, as  $\sigma$  vanishes only for our DFG model, the damped oscillations for the massive neutrino density contrast are not observed for the DFG during the radiation dominated era (ultra-relativistic period). In addition, since we have followed the above approach for matching DFG and neutrino energy densities one each other, the neutrino mass for a completely non-relativistic fluid is supposed to be given by  $m_\nu \approx 0.46 eV$ , while the DFG was already stated as  $m_d \approx 0.24 eV$ . For this reason the massive neutrinos become non-relativistic earlier. These two opposed effects compensated themselves so that the density contrast for massive neutrinos and for DFG have similar amplitudes at present.

The matter power spectrum for  $\Lambda\text{CDM} + \nu$  and  $\Lambda\text{CDM} + \text{DFG}$  universes are therefore very similar for large and small scales, with a small relative deviation for intermediate scales.

Fig. 6 shows the difference between the matter power spectrum for the cosmic inventories described at Table I. All the resulting matter power spectra were normalized to match one each other on large scales. Fig. 6 shows a certain level of decreasing on the  $\Lambda\text{CDM}$  power spectrum on small scales due to the introduction of an additional component into the cosmic inventory described by massless neutrinos, massive neutrinos or even a DFG. In fact, such a higher difference which is evident for small scales, when one compare the density contrast for CDM plus barions and for CDM plus barions modified by additional (exotic!?) cosmic fluids, has been discussed in some previous references [11].

Fig. 6 shows the difference between the matter power spectrum,  $P_m(k)$ , for the cosmic inventories described at Table I. The matter power spectrum is defined in the Fourier  $k$ -space as the averaged of the correlation function of the density contrast as

$$\langle \delta_m^\dagger(\vec{k}, \eta) \delta_m(\vec{k}', \eta) \rangle = (2\pi)^3 P_m(k) \delta^3(\vec{k} - \vec{k}'). \quad (73)$$

By observing that  $\delta_m = (\sum_i \bar{\rho}_i \delta_i) / (\sum_i \bar{\rho}_i)$  (all  $i$  matter components) and integrating the above equation over the solid angle  $d\Omega_k$ , one can depict the explicit value for  $P_m(k)$ . All the resulting matter power spectra were normalized to match one each other on large scales. Fig. 6 shows a certain level of decreasing on the  $\Lambda\text{CDM}$  power spectrum on small scales due to the introduction of an additional component into the cosmic inventory described by massless neutrinos, massive neutrinos or even a DFG. In fact, such a higher difference which is evident for small scales, when one compare the density contrast for CDM plus barions and for CDM plus barions modified by additional (exotic!?) cosmic fluids, has been discussed in some previous references [11].

Just to end up, in what concerns the neutrino degeneracy, one can ascertain that the value of the chemical potential of electron neutrinos ( $\mu_e/T_0$ ) should be close to  $-1$  in order to explain with an acceptable confidence level the phenomenology related to the observed variation of deuterium by roughly an order of magnitude [8]. It would induce a variation in total energy density during the radiation dominated stage, which is excluded by the smoothness of CMB. However, this objection could be avoided if there was a coincidence between different leptonic chemical potentials such that in different spatial regions they had the same values but with interchange of electronic, muonic and/or tauonic chemical potentials [20].

$\Omega$	without $\nu$	massless $\nu$	massive $\nu$	DFG
$\Omega_\Lambda$	0.73	0.73	0.73	0.73
$\Omega_\gamma$	4.6E-5	4.6E-5	4.6E-5	4.6E-5
$\Omega_b$	0.0425	0.0425	0.0425	0.0425
$\Omega_c$	0.2+r	0.2	0.2	0.2
$\Omega_r$	0	r	0	0
$\Omega_\nu$	0	0	r	0
$\Omega_d$	0	0	0	r

Table I: Cosmic inventory for obtain the matter power spectrum of Fig. 6. We did assume a flat universe  $\sum_i \Omega_i = 1$  or  $r = 0.027454$

For further details and discussion of energy dependence and effective chemical potential one might address the papers [20, 21] where the main point is that they are not obtrusive to our results.

## VI. CONCLUSIONS

The hypothesis of a small fraction of matter components evolving cosmologically as a DFG test fluid in some dominant cosmological background was evaluated through numerical and analytical approaches. Our proposal was based on the fact that for any type of fermionic dark matter, which includes relativistic and non-relativistic neutrinos, the average phase-space density cannot exceed the phase-space density of the DFG, which leads to the possibility of forming extended overdense regions of a fluid of degenerate particles. In the scope of our analysis, we have introduced some analytical procedures for obtaining the evolution of perturbations for a some categories of relativistic and non-relativistic test fluids. Expressions for the time evolution of the density contrast and the fluid velocity divergence with vanishing anisotropic stress  $\sigma$ , were obtained for a gas of massive and degenerate fermionic particles in the background regimes of radiation, matter, and cosmological constant dominated universes, and for super-horizon scales during the radiation-to-matter transition era.

Our primary results set that, during the period when the DFG could be approximated

by a ultra-relativistic gas, its density contrast presents an oscillating behavior similar to that of the photon perturbation during the radiation dominated era. Through analogous comparison with matter components, the freezing of DFG components leads to a combined linear plus logarithmic growing mode for the density contrast, similar to which one could obtain for CDM perturbations. Finally, during the  $\Lambda$  dominated era, the DFG perturbation terms are suppressed (as  $1/a$ ) due to the negative pressure of the dominant fluid.

Through numerical calculations, we have quantified the impact of a DFG component in the cosmic inventory on predictions for the matter power spectrum. It was performed by running the public code CAMB based on the synchronous gauge and comparing the results with the previous analytical studies based on the longitudinal gauge. For intermediate regimes, one could observe the suppression of the growing adiabatic modes which turns into a smoothly oscillatory behavior. Also for the fluid velocity divergence, the transition from ultra-relativistic to non-relativistic regimes was quantified. In this sense, our results has become a convenient tool for performing preliminary tests for HDM to CDM test fluid configurations. Being more specific, the effects quantified through analytical and numerical calculations and their relative impact on the cosmological structure formation were obtained by substituting the massive neutrino fluid by a DFG matter component. Assuming isentropic initial conditions, the Fermi momentum,  $q_F$ , and the mass value,  $m$ , were adjusted in order to give early (radiation dominated) and late (matter era) times averaged densities reproducing the cosmological background neutrino densities obtained through standard predictions for the  $\Lambda$ CDM model.

Generically speaking, the global evolution of the DFG perturbations obtained by numerical procedures is consistent with the analytical solutions. During the ultra-relativistic regime, the massive neutrino density contrast presents a damped oscillation while the power is transferred to higher multipoles. Obviously, through the approximation used for massive neutrinos, they become non-relativistic earlier than DFG since  $m < m_\nu$  for the same averaged densities. Meanwhile, the density contrast for the DFG and for massive neutrinos are very similar during the non-relativistic simultaneous regime (c. f. Fig. 5), even though it does not reach the growing rate of the CDM density contrast. The effects on the power spectrum for large and small scales ( $k\eta \ll 1$  and  $k\eta \gg 1$ ) are minimal if changing massive neutrinos by DFG. One of the subtle points of our analysis is that the effects on the matter power spectrum, due to the conversion of massive neutrinos into a DFG fluid in the cosmic

inventory, are relevant only for intermediary scales as depicted from Fig. 6.

To summarize, the reproducibility of our results through the conservation equations derived from the Bianchi identities, through the analytical approximations on the Boltzmann equation, and through the numerical calculations, ratifies the consistency of our analysis. Once the region of intermediate scales for the matter power spectrum are still open to theoretical speculations, our results could be extended to support the discussion of the formation of galaxy overdense regions of a gas of massive degenerate fermions in hydrostatic and thermal equilibrium at finite temperatures. A formulation that is consistent with the self-gravitating Fermi gas model introduced to explain the puzzling nature of white dwarf stars [15, 17].

### Acknowledgments

The authors would like to thank for the financial support from the Brazilian Agencies CAPES (Master Degree Program - IFGW), FAPESP (grant 08/50671-0) and CNPq (grant 300233/2010-8), and for the hospitality of the Department of Cosmic Rays and Chronology - IFGW - UNICAMP.

- 
- [1] Y. B. Zeldovich, *A & A* **5**, 84 (1970).
  - [2] L. Bergstrom, *Rept. Prog. Phys.* **63**, 793 (2000).
  - [3] G. Bertone, D. Hooper and J. Silk, *Phys. Rept.* **405**, 279 (2005).
  - [4] S. Calchi Novati, *Il Nuovo Cimento* **B122**, 557 (2007).
  - [5] C. L. Bennett *et al.*, *Astrophys. J. Suppl. Ser.* **148**, 1 (2003).
  - [6] D. Jeong and E. Komatsu, *Astrophys. J.* **651**, 619 (2006).
  - [7] S. Dodelson, *Modern Cosmology: Anisotropies and Inhomogeneities in the Universe*, (Academic Press, New York, 2003).
  - [8] A. D. Dolgov, *Phys. Rept.* **370**, 333 (2002).
  - [9] A. Boyarsky, A. Neronov, O. Ruchayskiy, and I. Tkachev, *Phys. Rev. Lett.* **104**, 191301 (2010).
  - [10] C. P. Ma and E. Bertschinger, *Astrophys. J.* **455**, 7 (1995).
  - [11] J. Lesgourgues and S. Pastor, *Phys. Rept.* **429**, 307 (2006).

- [12] A. E. Bernardini and O. Bertolami, Phys. Rev. **D81**, 123013 (2010).
- [13] N. Bilić and R. D. Viollier, Phys. Lett. **B408**, 75 (1997).
- [14] A. Dolgov and Ya B. Zel'dovich, Rev. Mod. Phys. **53**, 1 (1981).
- [15] S. Chandrasekhar, Ap. J **74**, 81 (1931); *An introduction to the Study of Stellar Structure*, (University of Chicago Press, 1939).
- [16] C. Cercignani and G. M. Kremer, *The relativistic Boltzmann equation: Theory and applications*, in *Progress in mathematical physics, Vol. 22*, (Birkhuser, Basel, Boston, 2002).
- [17] R. H. Fowler MNRAS **87**, 114 (1926).
- [18] A. E. Bernardini and E. L. D. Perico, JCAP **01**, 10 (2011).
- [19] A. Lewis and A. Challinor, *Code for Anisotropies in the Microwave Background*, <http://camb.info/>; A. Lewis, Ph.D. thesis, (Cambridge University, 2000), <http://cosmologist.info/thesis.ps.gz>; A. Challinor and A. Lasenby, Astrophys. J. **513**, 1 (1999); A. Challinor, Phys. Rev. **D62**, 043004 (2000); A. Lewis and A. Challinor, Phys. Rev. **D66**, 023531 (2002); A. Challinor and A. Lewis, Phys. Rev. **D71**, 103010 (2005).
- [20] W. Hu and J. Silk, Phys. Rev. Lett. **70**, 2661 (1993).
- [21] W. Hu and J. Silk, Phys. Rev. **D48**, 485 (1993).

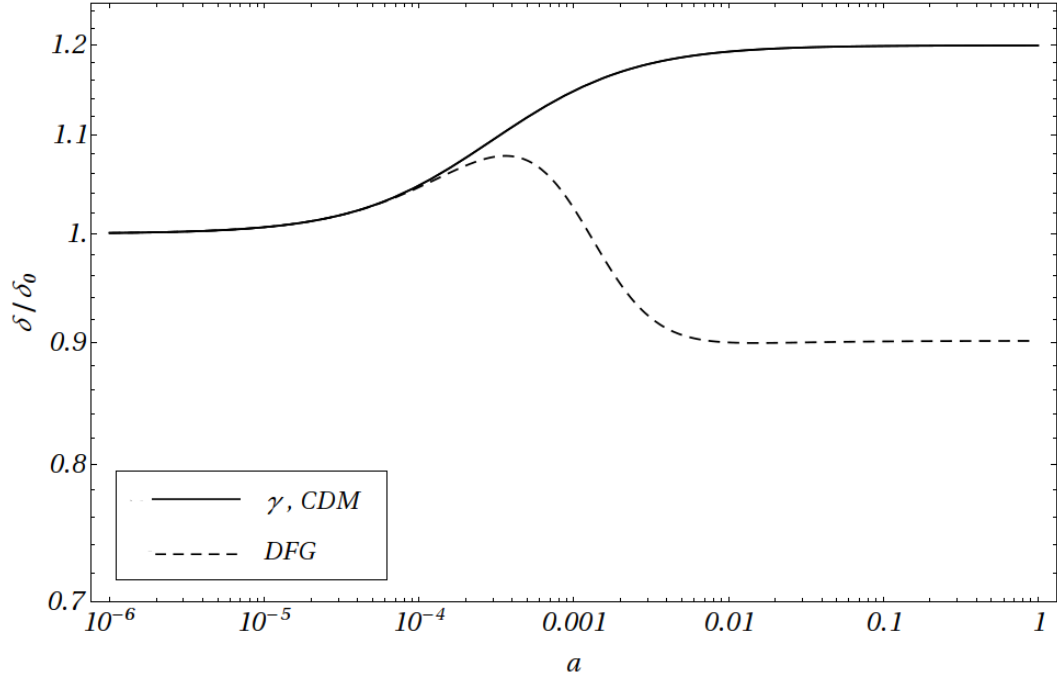


Figure 1: Growing mode of the density contrast  $\delta$  for  $DFG$ , radiation and  $CDM$  at super-horizon approximation (i. e.  $k\eta \ll 1$ ) in dependence on the scale parameter,  $a$ . The plots correspond to analytical solutions in the longitudinal gauge for radiation and matter dominated universes.

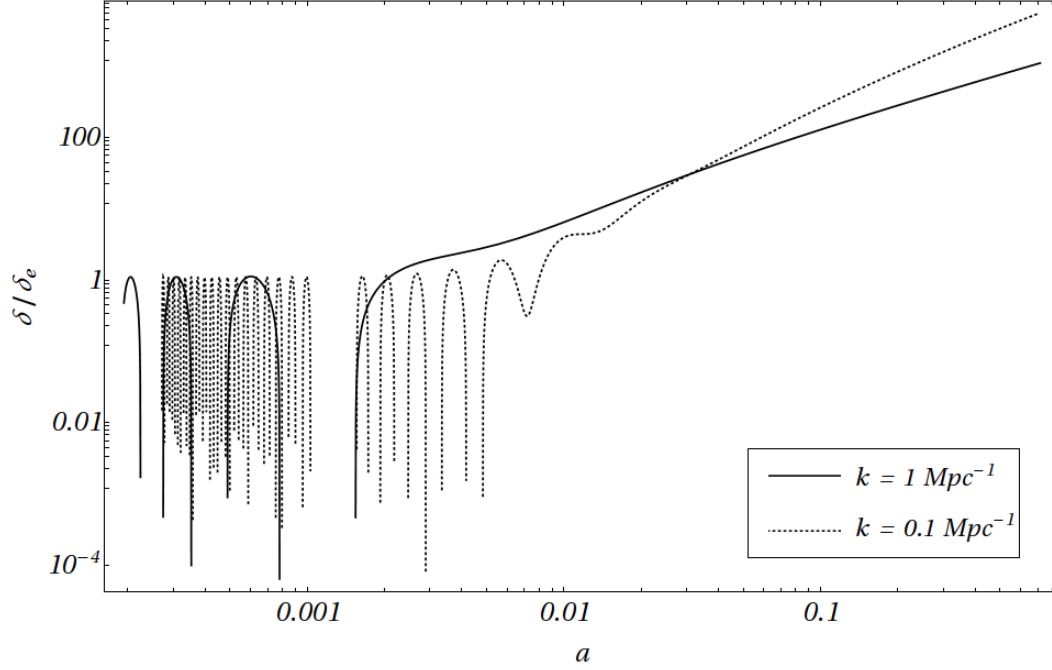


Figure 2: Analytical results for the growing mode of the DFG density contrast,  $\delta$ , during the matter dominated era as function of the scale parameter,  $a$ . The calculations were performed in the longitudinal gauge for two different scales parameterized by the wavenumber  $k$ ;  $k = 0.1 \text{ Mpc}^{-1}$  and  $k = 1 \text{ Mpc}^{-1}$ .

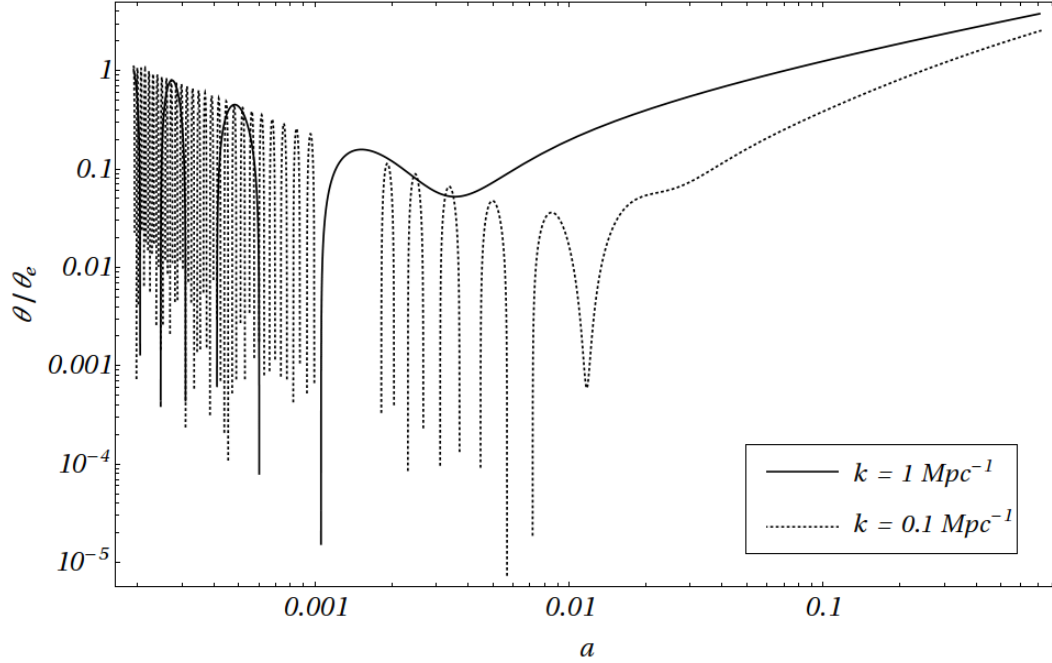


Figure 3: Analytical results for the growing mode of the DFG velocity divergence,  $\theta$ , during the matter dominated era as function of the scale parameter,  $a$ . The calculations were performed in the longitudinal gauge for  $k = 0.1 \text{ Mpc}^{-1}$  and  $k = 1 \text{ Mpc}^{-1}$ .

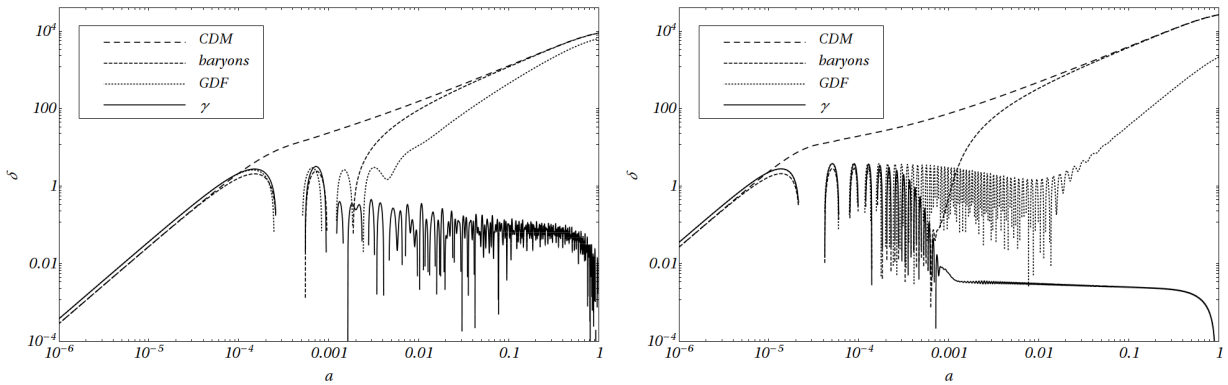


Figure 4: Numerical results for the density contrast,  $\delta$ , (in the synchronous gauge) for  $CDM$ , baryons,  $DFG$  and photons as function of the scale parameter,  $a$ . The calculations were performed in the longitudinal gauge for two different scales parameterized by the wavenumber  $k$ ;  $k = 0.1 \text{ Mpc}^{-1}$  (left) and  $k = 1 \text{ Mpc}^{-1}$  (right).

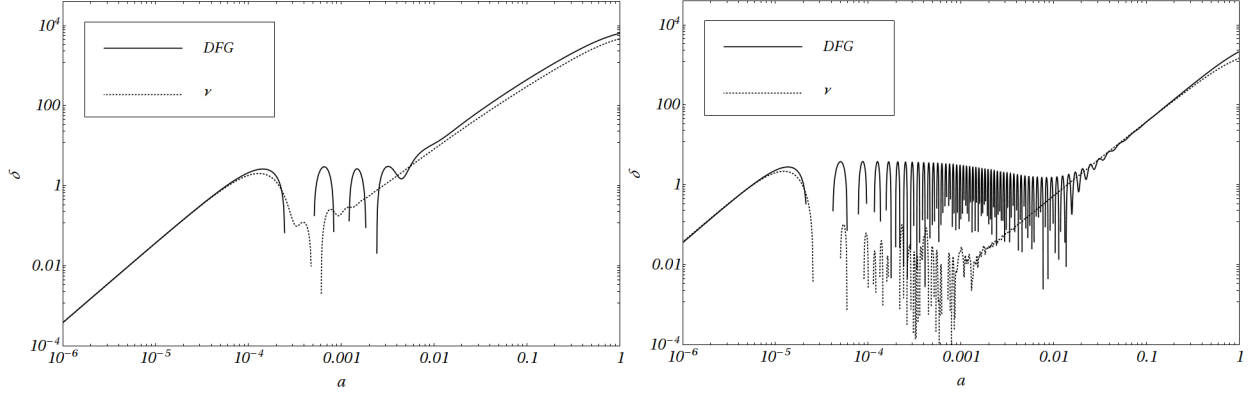


Figure 5: Comparison between the massive neutrino density contrast and the  $DFG$  density contrast in dependence on the scale parameter,  $a$ . It is assumed the same initial and final averaged densities for both fluids (the last two columns on table I). For completeness, the wavenumber here assumed are  $k = 0.1 \text{ Mpc}^{-1}$  (left) and  $k = 1 \text{ Mpc}^{-1}$  (right).

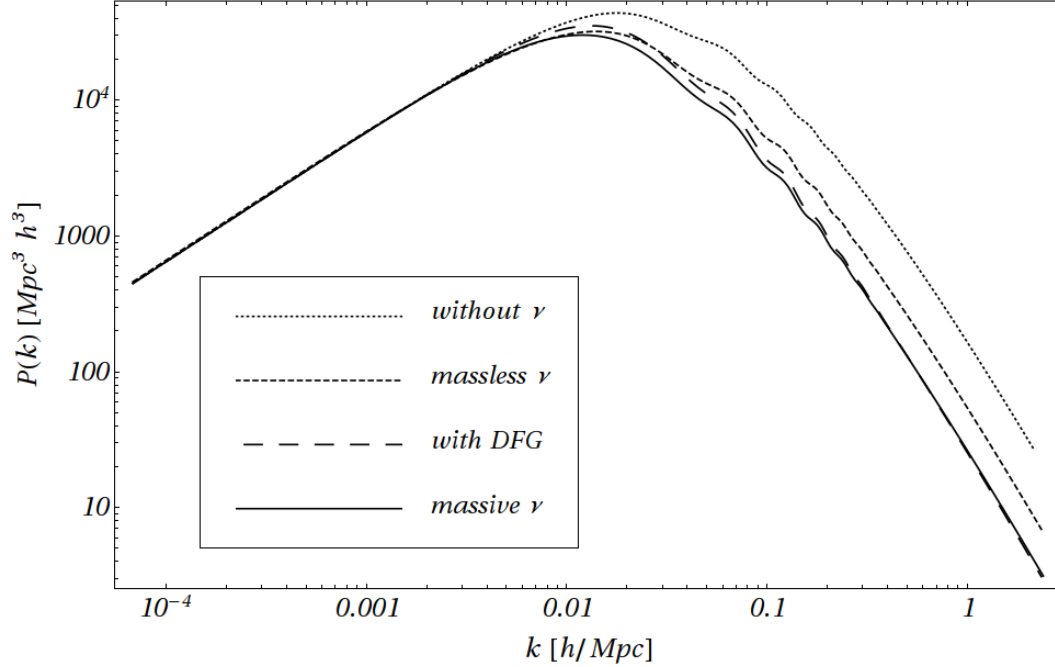


Figure 6: Matter power spectrum  $P(k)$  according to the cosmic inventory described by the components of table I in the  $\Lambda\text{CDM}$  background scenario.